

Frequency-dependent heat transfer enhancement from rectangular heated block array in a pulsating channel flow

Jeong Woo Moon ^a, Seo Young Kim ^{a,*}, Hyung Hee Cho ^b

^a *ThermalFlow Control Research Center, Korea Institute of Science and Technology, P.O. Box 131, Cheongyang, Seoul 130-650, Republic of Korea*

^b *Department of Mechanical Engineering, Yonsei University, Seoul 120-840, Republic of Korea*

Received 2 July 2004; received in revised form 27 March 2005

Available online 10 August 2005

Abstract

The effect of pulsating flow on convective heat transfer from periodically spaced blocks in tandem on a channel wall is experimentally investigated. The spacing l between repeated blocks varied from $l/L = 0.3$ to 0.6 where L is the block pitch. The experiments are carried out in the range of $10 \text{ Hz} < f_F < 100 \text{ Hz}$ and $0.2 < A < 0.3$. A pulsating flow is imposed by an acoustic woofer at the channel inlet and a constant heat is generated at each protruding block. The impact of the important governing parameters such as the Reynolds number, the Strouhal number and the inter-block spacing on heat transfer rate from heated blocks is examined in detail. The experimental results show that thermal transport from the blocks is greatly affected by the frequency, the amplitude of the flow pulsation, the inter-block spacing and the Reynolds number. Thermal resonance frequency which shows a maximum heat transfer coincides well with the inverse of traveling time of a fluid parcel that can be determined from the block periodicity and the Reynolds number.

© 2005 Elsevier Ltd. All rights reserved.

1. Introduction

Extensive studies on heat transfer from a heated block array in a channel have been conducted in response to industrial demand such as electronics cooling and compact heat exchangers. For the steady flow, lots of experimental and numerical studies [1–6] showed that as fluid passed over a heated block array, the periodic

redevelopment of thermal boundary layer occurred at each block and its contribution was crucial to the total heat transfer rate. Inside the inter-block region, however, heat transfer was relatively meager attributed to less flow communication of recirculating cell with the main throughflow.

In an effort to enhance convective heat transfer from such a confined recirculation zone, a heat transfer augmentation scheme adding a pulsation component to a main through-flow has been proposed in recent years. This scheme was relevant to the amplification of the flow instability inherently existed in a self-sustained oscillation regime by forced pulsation [7–12]. Using the flow

* Corresponding author. Tel.: +82 2 958 5683; fax: +82 2 958 5689.

E-mail address: seoykim@kist.re.kr (S.Y. Kim).

Nomenclature

<i>a</i>	height of a block [mm]	<i>St</i>	Strouhal number, fH/U_o
<i>A</i>	oscillating amplitude of axial velocity	<i>St_F</i>	Strouhal number of inlet pulsating frequency, $f_F H/U_o$
<i>D</i>	length of a block [mm]	<i>St_R</i>	Strouhal number of thermal resonance frequency, $f_R H/U_o$
<i>G</i>	geometry	<i>T</i>	local temperature [K]
<i>E</i>	heat transfer enhancement factor, Nu_p/Nu_s	<i>T_a</i>	inlet air temperature [K]
<i>f</i>	dimensional frequency [Hz]	<i>T_b</i>	bulk air temperature [K]
<i>f_F</i>	forcing frequency of pulsating flow [Hz]	<i>U_c</i>	time-averaged velocity at the channel center over the block array, $(3/2)(\bar{Q}/2hW)$ [m/s]
<i>f_n</i>	natural shedding frequency of a block array [Hz]	<i>U_i</i>	inlet velocity, $U_i = U_o(1 + A \sin 2\pi f_F t)$ [m/s]
<i>f_R</i>	thermal resonance frequency at which the resonance in heat transfer occurs [Hz]	<i>U_o</i>	time-averaged velocity of the inlet flow [m/s]
<i>h</i>	half height of flow channel above the block [mm]	<i>U_p</i>	oscillatory amplitude of inlet velocity, $U_o \cdot A$ [m/s]
<i>h_c</i>	convective heat transfer coefficient [W/m ² K]	<i>W</i>	Channel width [m]
<i>H</i>	height of flow channel [mm]		
<i>k</i>	thermal conductivity [W/m K]	<i>Greek symbols</i>	
<i>l</i>	inter-block spacing [mm]	<i>v</i>	kinematic viscosity [m ² /s]
<i>L</i>	block pitch [mm]	<i>τ</i>	characteristic frequency estimated by convective time scale, $τ = L/U_c$ [Hz]
<i>Nu</i>	time-averaged local Nusselt number at each block, $Nu = h_c H/k = qH/(T - T_a)k$	<i>Subscripts</i>	
<i>Nu_b</i>	time-averaged local bulk Nusselt number at each block, $Nu_b = qH/(T - T_b)k$	<i>G</i>	previous study by Greiner [7]
\bar{Q}	time-averaged flow rate [m ³ /s]	<i>N</i>	previous study by Nishimura et al. [9]
<i>q</i>	heat flux input at the heated block surface [W/m ²]	<i>p</i>	pulsating component
<i>Re_H</i>	Reynolds number, $U_o H/\nu$	<i>s</i>	steady-state component

pulsation, the amplified hydrodynamic instability in a shear layer substantially augmented flow mixing in a channel, and resulted in convective thermal transport enhancement. Ghaddar et al. [7,8] showed that the least stable mode existed in a periodic grooved-channel flow and heat transfer was augmented when the pulsation frequency was in tune with a specific frequency of the least stable mode, which was indicative of resonance. This resonant phenomenon in heat transfer was experimentally verified by Greiner [9]. Kim et al. [10] carried out numerical studies for the pulsating flow and the associated heat transfer from two successive heated blocks inside a channel and reported that heat transfer was enhanced by spatially enhanced flow mixing with the presence of pulsation. Nishimura et al. [11] studied fluid mixing and mass transfer in a grooved channel with different inter-block spacings. Recently, Bae et al. [12] demonstrated the resonant convective heat transfer augmentation at downstream protruding blocks by controlling time-periodic change of heat generation rate at the most upstream block in a multi-block arrangement.

Some studies [7–9] revealed that small fluid oscillation with the natural frequency of the hydrodynamic instability amplified the flow instability within a grooved

channel, even at Reynolds numbers below the critical value for the onset of self-sustained oscillations, and thus enhanced heat transfer. The natural frequency was closely matched with the Tollmien–Schlichting wave for the grooved channel [7,8]. However, some previous experimental works showed that thermal resonance frequency did not always coincide with the natural frequency estimated by the hydrodynamic instability wave. Nishimura et al. [11] raised such a question that the resonance mechanism in a grooved channel was not clearly explained by the Tollmien–Schlichting wave for some cases. Therefore, there seems to be another dominant frequency which characterizes resonant heat transfer enhancement in a pulsating grooved channel flow.

The present paper examines experimentally the influence of pulsation frequency on the convective heat transfer from a heated block array as shown in Fig. 1. Based on the present experimental data, the resonant frequency for convective heat transfer enhancement will be evaluated, comparing with the results based on the previous hydrodynamic instability concept. Finally, we aim to elucidate thermal resonance mechanism from a heated block array by the flow pulsation.

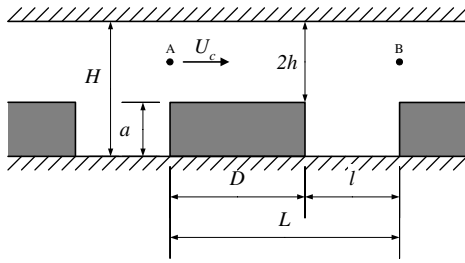


Fig. 1. Schema of a heated block array in a channel.

2. Experimental setup and test procedure

A rectangular channel of cross-sectional area of 180 mm (W) \times 20 mm (H) and of 800 mm in length was made of 5 mm thick Plexiglas plates. A steady main airflow was supplied through a rotameter via a pressure regulator from an air compressor. Three-stage mesh screens and a honeycomb were installed to produce a uniform inlet flow with low turbulence intensity as displayed in Fig. 2. The turbulence intensity was about 0.37% for the steady flow at $Re_H = 700$.

A 190 mm-woofer was installed to a cone-shaped chamber to produce an oscillatory flow. The conical chamber for the woofer was connected to an air-mixing plenum upstream of the channel with a flexible tube to eliminate transmission of structural vibration. A function generator (HP-33120A) provided a sinusoidal signal with a prescribed frequency, and then the signal was amplified by a signal amplifier (Inkel, AX7030G). The amplified signal was sent to the woofer via a digital oscilloscope (LeCroy, 9310A) to check the input frequency and voltage. The time-variant pulsating velocity at the mid portion of the channel inlet was measured by a hot-wire anemometry (Kanomax, IHW-100). Fig. 3

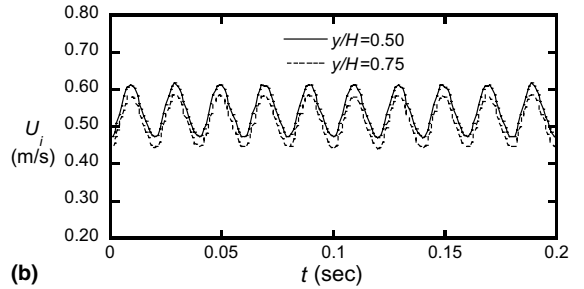
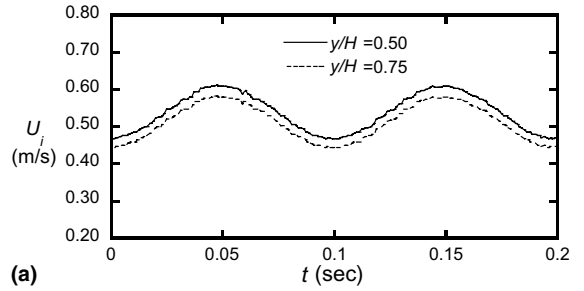


Fig. 3. The measured inlet velocity U_i at $Re_H = 700$ and $A = 0.2$. (a) $f_F = 10$ Hz and (b) $f_F = 50$ Hz.

shows the time-variant inlet pulsating velocity for two different pulsation frequencies: $f_F = 10$ Hz and 50 Hz. The figures demonstrate that the present acoustic excitation can provide sinusoidal flow-pulsations.

For the internal pulsating flow, the Womersley number, $Wo = H/2(2\pi f/\nu)^{1/2}$, is generally used to describe the unsteady characteristic of fluid flow in response to unsteady pressure gradient. When $Wo > 10$, the velocity profile becomes almost uniform and in-phase in the core [13]. For all the flow conditions used in this study, Wo was much larger than 10. Therefore, the inlet velocity

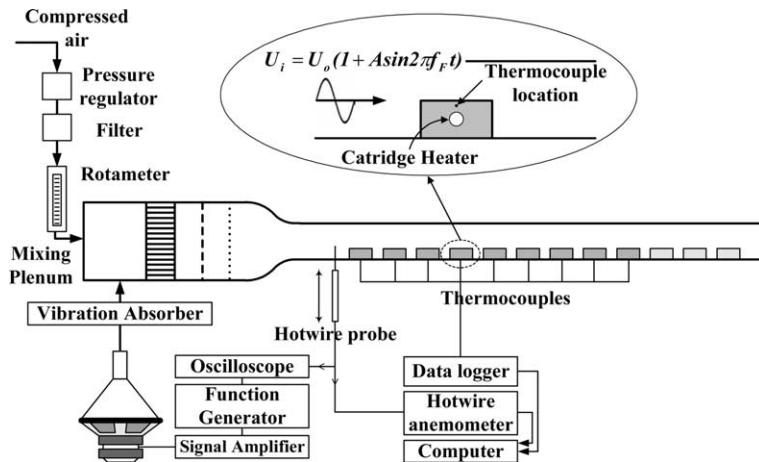


Fig. 2. Experimental setup.

measured at the channel center might represent the flow characteristic of the inlet pulsation. As shown in Fig. 3, the uniformity of the vertical velocity profile is little changed by the elevation of the measurement.

Nine rectangular blocks made of aluminum of 10 mm (a) \times 20 mm (D) \times 180 mm (W) were mounted on the bottom of the channel. To compare the present experimental results with the previous data and identify the effect of the block height, rectangular blocks of 9 mm (a) \times 37 mm (D) \times 180 mm (W), 8.8 mm (a) \times 26.2 mm (D) \times 180 mm (W), 8.8 mm (a) \times 35 mm (D) \times 180 mm (W) and 15 mm (a) \times 20 mm (D) \times 180 mm (W) were also fabricated. The geometric particulars for the present experiment are given in Table 1. G_G and G_N denote the experimental geometries of Greiner [9] and of Nishimura et al. [9], respectively. To reproduce the Greiner's study with the same geometry, the height of the flow channel is modified into $H = 19.5$ mm. To provide a uniform heat generation from the blocks, a cylindrical cartridge heater was inserted into the center hole fabricated on each block and then it was fixed using a thermal compound. The heaters were controlled by a DC power supply. T-type thermocouples (Omega Scientific, AWG 36) were attached on the top surfaces of the blocks. To estimate conduction heat loss through the bottom wall, ten pairs of thermocouples were attached to the bottom of the channel wall. The total estimated heat loss was about 13.2% for $Re_H = 700$.

The experiment was started by heating up the heaters and supplying cold air into the channel without imposing the flow pulsation. The steady-state temperature data were collected by a data acquisition system (Yokogawa, DR-230) and stored in a PC. After collecting the steady-state temperature data, the pulsating flow was imposed by the acoustic woofer. In the present study, the pulsation frequency was varied in the range of 10–100 Hz and the velocity amplitude of the pulsation from $A = 0.2$ to 0.3. The time-varying flow velocity was measured at the inlet by a hot-wire anemometer during the flow pulsation to determine the pulsating velocity amplitude and the Reynolds number. After reaching a

time-periodic quasi steady-state, temperature data were stored in the data acquisition system for analysis.

To measure the vortex shedding frequency generated from the protruding blocks, a hot-wire probe was installed downstream of $D/5$ from the backward-facing surface of the seventh block and at the height of $1.0a$ from the bottom wall. The measured time signal of the fluctuating velocity was sent to the digital oscilloscope to perform the Fast Fourier Transform (FFT). The FFT data clearly provided the vortex shedding frequency generated from the heated block array.

3. Data reduction

Typically, three flow parameters characterize the pulsating flow: the mean flow Reynolds number, the amplitude of the velocity pulsation and the Strouhal number

$$Re_H = \frac{U_o H}{\nu} \tag{1}$$

$$A = \frac{U_p}{U_o} \tag{2}$$

$$St_F = \frac{f_F H}{U_o} \tag{3}$$

where U_o denotes the time-averaged inlet flow velocity, U_p is the magnitude of the inlet velocity pulsation. The Nusselt number Nu at each block is expressed in terms of the given heat flux and the measured surface temperature. Thus,

$$Nu = \frac{h_c H}{k} = \frac{q_{conv} H}{k(T - T_a)} \tag{4}$$

$$Nu_b = \frac{q_{conv} H}{k(T - T_b)} \tag{5}$$

$$q_{conv} = q - q_{cond} \tag{6}$$

Here, q is supplied by the electrical cartridge heater. q_{cond} is the heat loss conducted through the bottom wall.

The uncertainties in the present experimental results were estimated by the single-sample experiment analysis by Kline and McClintock in Ref. [14]. For instance, the uncertainty in the Nusselt number, $\delta Nu/Nu$, could be obtained from Eq. (4):

$$\frac{\delta Nu}{Nu} = \left[\left(\frac{\delta q_{conv}}{q_{conv}} \right)^2 + \left(\frac{\delta(T - T_a)}{T - T_a} \right)^2 + \left(\frac{\delta H}{H} \right)^2 + \left(\frac{\delta k}{k} \right)^2 \right]^{1/2} \tag{7}$$

Here, the contribution by the geometrical parameters such as H to the overall uncertainty was negligible. Therefore, the estimated uncertainty for the Nusselt numbers for the steady flow was about 6.2% at $Re_H = 700$ in 95% confidence level. For the pulsating flow, the uncertainty was estimated about 7.4% at $Re_H =$

Table 1
Block array geometric particulars

Geometry	l/L	L/H	D/a	a/H
G_1	0.33	1.50	2.00	0.5
G_2	0.50	2.00	2.00	0.5
G_3	0.66	3.00	2.00	0.5
G_4	0.50	2.00	1.33	0.75
G_G [9]	0.33	2.80	4.08	0.46
G_{G1} [9]	0.32	2.80	4.11	0.46
G_{G2}	0.50	3.79	4.11	0.46
G_{G3}	0.60	4.75	4.11	0.46
G_{N1} [11]	0.33	2.62	3.97	0.44
G_{N2} [11]	0.50	2.62	2.97	0.44

700. Similarly, the uncertainty in Re_H was estimated to be 3.8% attributed to 3.1% in u and 2.2% in v .

4. Results and discussion

Heat transfer characteristics from the heated block array for the non-pulsating steady flow at $Re_H = 700$ are exemplified in Fig. 4. Three different block geometries (G_1, G_2 and G_3) are used to describe the effect of inter-block spacing on heat transfer. The present experimental results are compared with the numerical

data of Young and Vafai [5] for the forced convection in a channel with heated blocks. Fig. 4(a) exemplifies the Nusselt numbers at the steady-state for the geometries of G_1, G_2 and G_3 . Generally satisfactory agreement is apparent between the experimental results and the previous data. The Nusselt number Nu_b based on the bulk temperature is also displayed in Fig. 4(b), which is compared with the experimental results of Farhanieh et al. [3] and the numerical results of Furukawa and Yang [6]. The Nusselt number values Nu_b are in accordance with the previously reported results [3,6] for slightly different geometry and Reynolds number range. As shown in Fig. 4(b), the value of Nu_b remains almost constant beyond the fifth block of the array for all the inter-block spacing of the block array. This means that the flow over the block array reaches a periodically and fully developed region after the fifth block of the array. As the inter-block spacing increases, heat transfer from downstream blocks is substantially pronounced. The increase in l/L enhances cold flow entrainment to hot recirculation zone formed between the blocks and yield augmented heat transfer. Heat transfer enhancement with the increase of the inter-block spacing may be also attributed to the onset of the self-sustained oscillation [11].

Fig. 5 displays the frequency spectrum for the velocity fluctuation measured downstream of the seventh block. The hot-wire probe is installed at the downstream location of $D/5$ from the backward-facing surface of the seventh block and at the height of $1.0a$ from the bottom wall. As shown in Fig. 5, there is no significant vortex shedding for the block array with a small inter-block spacing ($l/L = 0.33$) in Fig. 5(a) while clear vortex shedding is observed for larger inter-block spacings ($l/L \geq 0.5$) in Fig. 5(a) and (c). The critical Reynolds number for the onset of self-sustained oscillation depends on the inter-block spacing, which becomes smaller as the inter-block spacing increases [11]. When $l/L = 0.5$, the critical Reynolds number is $Re_c \sim 450$ in the present study. The augmented velocity fluctuation beyond the critical Reynolds number yields heat transfer enhancement owing to increased flow mixing near the block surface and inside the inter-block region. Therefore, the heat transfer rate for larger inter-block spacings could be much higher than that for $l/L = 0.33$. It is also interesting to note that the shedding frequency decreases as l/L increases.

The influence of the flow pulsation on heat transfer from the heated block array will be dealt with hereafter. The Nusselt number and the associated heat transfer enhancement factor E at each block for the pulsating flow at $Re_H = 700$ are displayed in Figs. 6–8. The pulsation amplitude is fixed at $A = 0.2$, and three different inter-block spacings are considered here: $l/L = 0.33$ (G_1), 0.50 (G_2) and 0.66 (G_3). The heat transfer enhancement factor E is defined as the ratio of Nu_p to Nu_s .

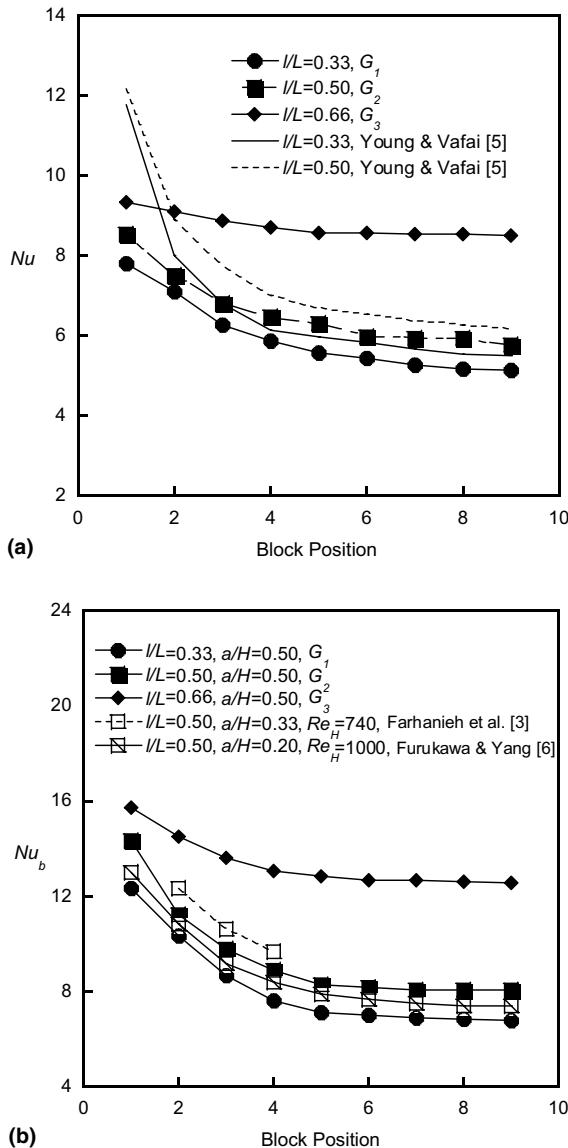


Fig. 4. (a) Nusselt number and (b) bulk Nusselt number at each heated block for the steady flow at $Re_H = 700$.

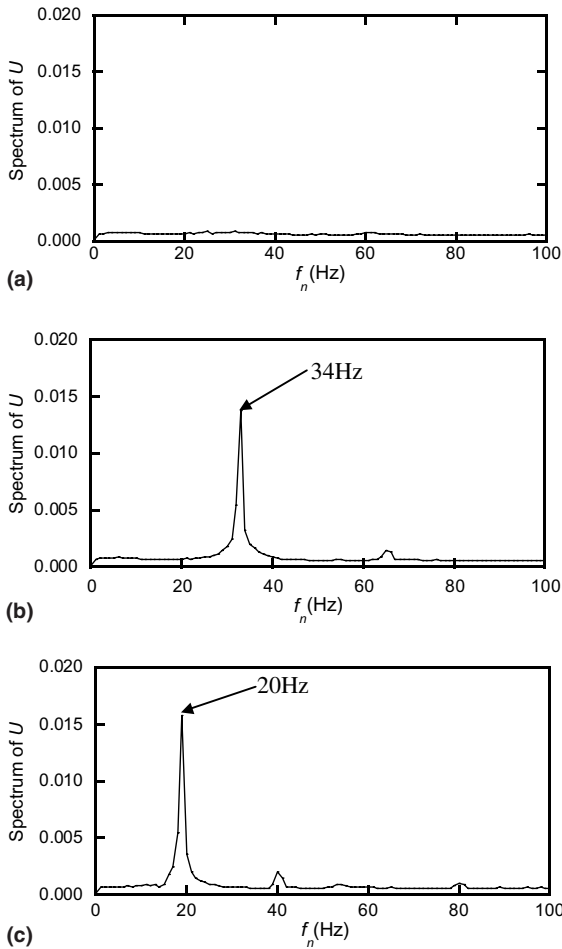


Fig. 5. Power spectrum of vortex shedding frequency measured downstream of the seventh block. $Re_H = 700$. (a) $l/L = 0.33$, $L/H = 1.5$: G_1 , (b) $l/L = 0.50$, $L/H = 2.0$: G_2 and (c) $l/L = 0.66$, $L/H = 3.0$: G_3 .

Fig. 6 shows the variation of the Nusselt number Nu and the enhancement factor E for various f_F when $l/L = 0.33$. When the pulsating component is added to the main through-flow, heat transfer is generally enhanced by vigorous fluid communication between the cold mainstream and the recirculation flow inside the inter-block region. For $l/L = 0.33$, however, the inter-block spacing is too small for the cold mainstream to infiltrate into the inter-block region. Therefore, heat transfer enhancement is relatively meager compared to that for larger inter-block spacings. The enhancement factor at the most upstream block shows a peak around $f_F = 40$ Hz while those at downstream blocks are maximized at around $f_F = 55$ Hz. In addition, heat transfer from the 1st block maintains enhancement even beyond the thermal resonance frequency of $f_F \sim 40$ Hz, which is not in accordance with the heat transfer characteristics

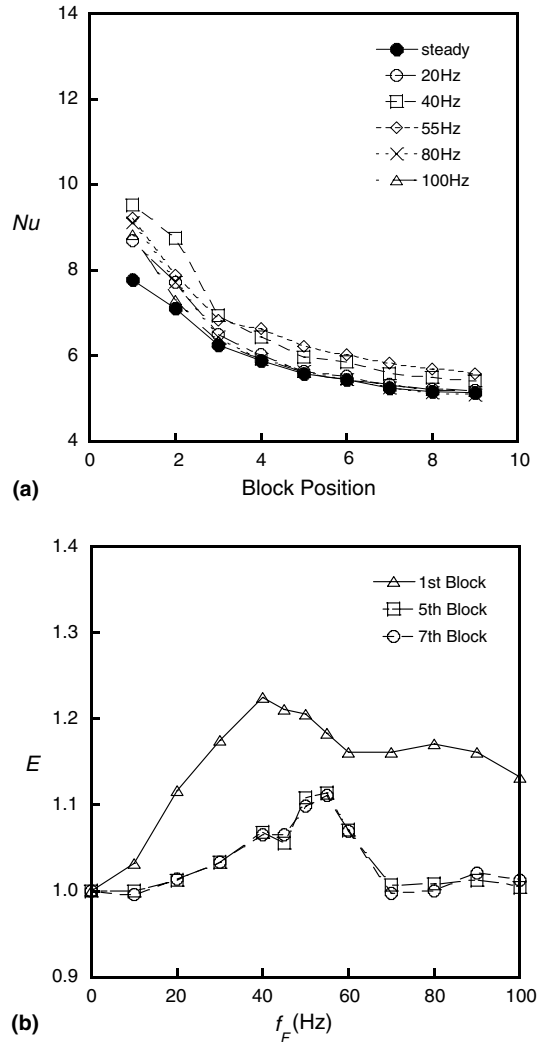
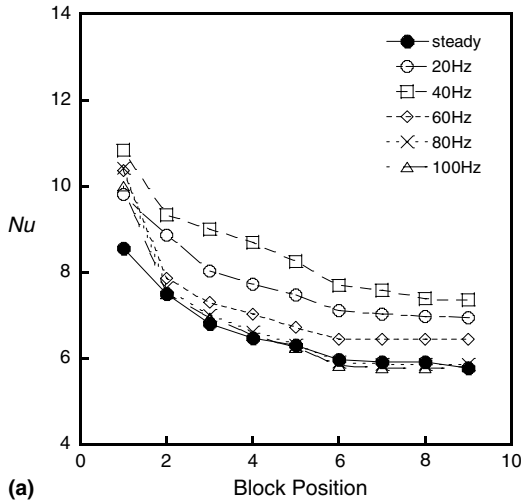


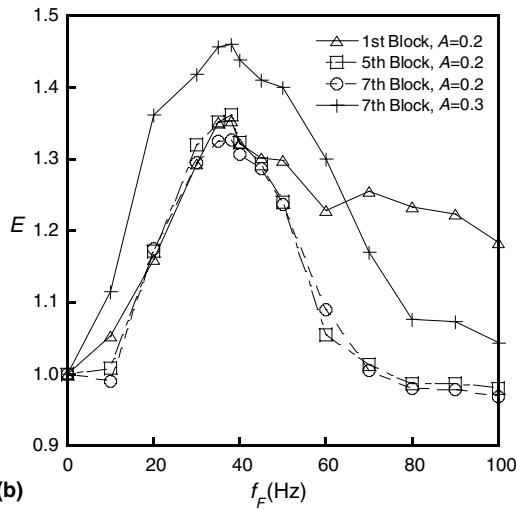
Fig. 6. The variation of (a) Nusselt number at each block and (b) heat transfer enhancement factor for G_1 . $Re_H = 700$ and $A = 0.2$.

of downstream blocks. For the downstream blocks, E drops down to 1.0 beyond thermal resonance frequency of $f_F \sim 55$ Hz.

The Nusselt number Nu and heat transfer enhancement E for $l/L = 0.5$ at $Re_H = 700$ are plotted in Fig. 7. The heat transfer is considerably augmented at all the blocks. Thermal resonance frequency at the fifth and seventh blocks decreases to $f_F = 38$ Hz as the inter-block spacing increases up to $l/L = 0.5$. The general trend of heat transfer at the 1st block is the same as that for a narrow spacing of $l/L = 0.33$ in Fig. 6(b). The effect of the velocity amplitude A on the heat transfer enhancement at the seventh block is shown in Fig. 7(b). As the velocity amplitude increases, heat transfer is more pronounced. However, thermal resonant frequency of



(a)

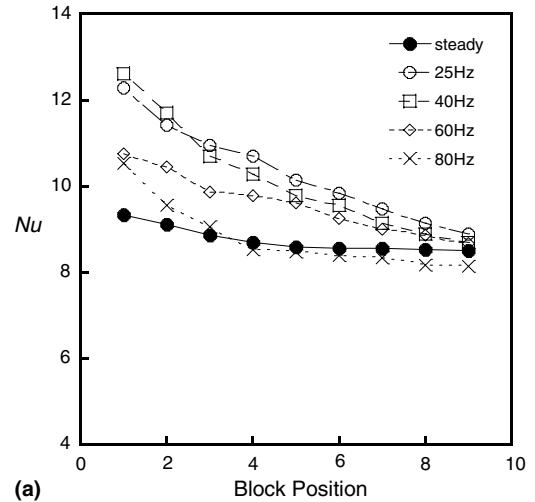


(b)

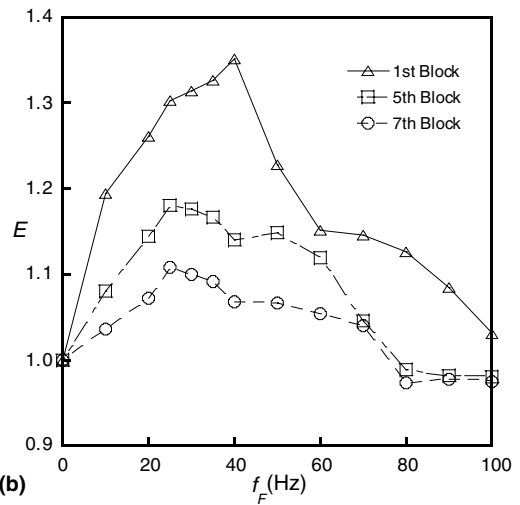
Fig. 7. The variation of (a) Nusselt number at each block and (b) heat transfer enhancement factor for G_2 . $Re_H = 700$.

$f_F \sim 38$ Hz is little affected by the increase of the velocity amplitude. This trend is in good agreement with the previous findings [10].

Fig. 8 displays Nu and E for $l/L = 0.66$ at $Re_H = 700$. With the increase of the pulsating frequency, heat transfer is mainly augmented at upstream blocks. The block array with a large inter-block spacing shows higher Nu for the steady flow. When the inter-block spacing is large ($l/L = 0.66$), however, the heat transfer enhancement by the pulsating flow is less effective since the effect of cold fluid entrainment into the inter-block region is very strong even for the steady flow, which results in higher Nu . The enhancement factor at the most upstream block shows a peak around $f_F = 40$ Hz while that at downstream blocks is maximized at around $f_F = 25$ Hz. When the pulsation frequency of the inlet flow matches a char-



(a)



(b)

Fig. 8. The variation of (a) Nusselt number at each block and (b) heat transfer enhancement factor for G_3 . $Re_H = 700$ and $A = 0.2$.

acteristic frequency of a system, substantial augmentation in heat transfer takes place, which is referred to as thermal resonance from now on.

Fig. 9 displays the effect of the block height on the heat transfer enhancement at the seventh block. The block geometric particulars are set to $l/L = 0.5$ and $L/H = 2.0$. The block height varies from $a/H = 0.50$ (G_2) to $a/H = 0.75$ (G_4). The flow velocity over the block array is set to be equal each other for two different height of the block. It indicates that the Reynolds number is $Re_H = 700$ for $a/H = 0.50$ and $Re_H = 350$ for $a/H = 0.75$, respectively. As the block height increases, heat transfer enhancement factor from the block is somewhat reduced. However, the thermal resonant frequency is little changed by the increase of the

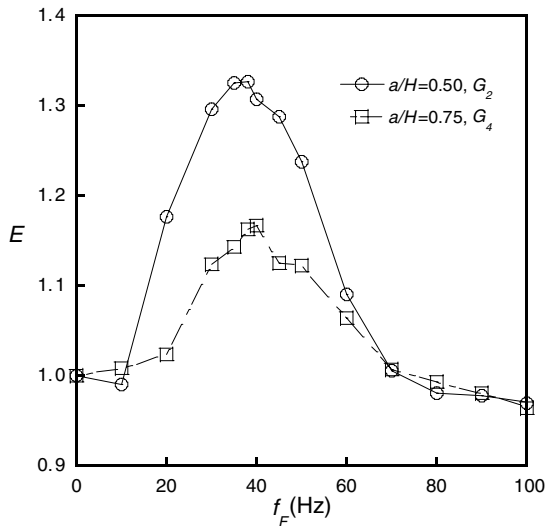


Fig. 9. Effect of block height on heat transfer enhancement for G_2 and G_4 .

block height. This means that thermal resonance frequency is invariant if the flow velocity over the block array is identical.

As seen from the experimental results in Figs. 6–8, the thermal resonance frequency is affected by the variation of the block array geometry. For a grooved channel, Refs. [7,8] attempted to estimate thermal resonance frequency by the linear stability theory. However, the analytical prediction of this characteristic frequency by the linear stability theory may not be easily obtained due to the lack of information on the wave number of the flow system. Furthermore, it was reported that the estimated frequency based on the stability theory showed some discrepancy compared to the experimental data [11]. As mentioned earlier in Fig. 5(b), the flow for $l/D = 1.0$ is already in a self-sustained oscillation regime. According to the experimental results, however, thermal resonance frequency observed is somewhat different from the natural shedding frequency in this flow regime. This means that the amplified hydrodynamic instability by the flow pulsation may be not responsible for heat transfer enhancement from the grooved channel. Therefore, we can postulate that there is another dominant frequency to characterize thermal resonance in a pulsating channel flow. We here now suggest a new concept to estimate the characteristic frequency at which thermal resonance occurs. The geometry used in this study has the arrangement of repeated blocks in tandem. If the flow over the block array reaches a periodically and fully developed region, we can evaluate the traveling time of the flow that passes over a periodicity with a block and an inter-block region. It means that the flow system has a characteristic frequency which is defined as the

reciprocal of the traveling time. In this study, we set the length of periodicity L in Fig. 1 and define the traveling time as $\tau = L/U_c$ where U_c is the characteristic velocity over the block array. To compare the previous frequency selection method with the present traveling time concept, first of all, the experimental results are reproduced for the same geometries as in Refs. [9,11]. Heat transfer enhancement factor E is measured at the seventh block in the fully developed region. Then, the experimental data are compared with the estimation results by the present traveling time concept, the linear stability theory [9] and the measured vortex shedding frequency.

The experiment was performed for the same geometry (G_{G1}) and the flow condition ($Re_H = 700$ and $A = 0.2$) used in Greiner [9]. Fig. 10 demonstrates that the present experimental results are in good accordance with the experimental results obtained by Greiner [9] in the viewpoint of the thermal resonant frequency. Both the experimental results in Fig. 10 show that the thermal resonance occurs at $St_F \sim 1.16$. However, the result in Greiner [9] shows much higher heat transfer enhancement than the present experimental data. This may be attributed to geometrical difference. For the Greiner’s study, heat is generated from all the grooved channel surfaces while it is generated only from the block surface in this study. The heat transfer enhancement by the pulsating flow in a grooved channel mainly occurs at the inter-block region so that heat transfer augmentation in Greiner’s experiment is more substantial.

Comparison of thermal resonance frequency between the estimation results by the traveling time concept and the experimental data is made in Fig. 11. The experiments

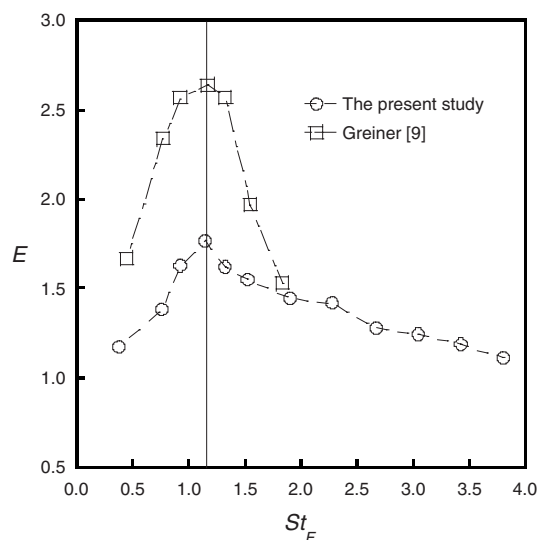


Fig. 10. Heat transfer enhancement factor as a function of St_F for G_{G1} [9] at $Re_H = 700$ and $A = 0.2$.

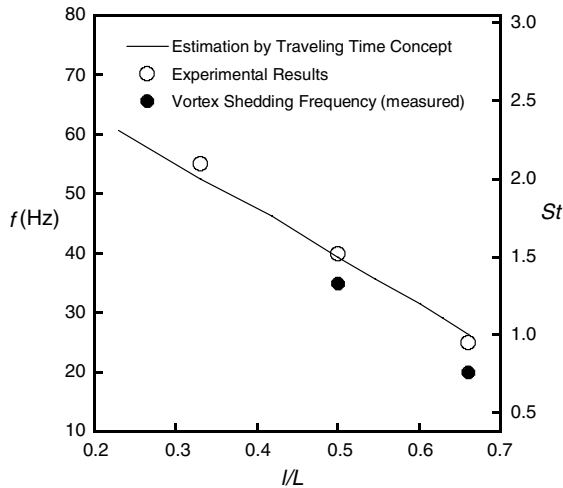


Fig. 11. The effect of block spacing on thermal resonance frequency for $D/a = 2.0$ and $a/H = 0.5$ at $Re_H = 700$ and $A = 0.2$.

and the predictions have been performed for the geometries of G_1, G_2 and G_3 listed in Table 1. The experimental results show that the thermal resonance frequency decreases with the increase of inter-block spacing. The natural shedding frequency measured from the block array also shows a similar trend to the experimental results. However, the estimated characteristic frequency based on the traveling time concept displays better agreement with the experimental results.

Fig. 12 shows thermal resonance frequency for the geometry used in Ref. [9] at $Re_H = 700$. The pulsation amplitude is fixed at $A = 0.2$. The experiments and the predictions have been performed for G_{G1}, G_{G2} and G_{G3} listed in Table 1. The inter-block spacing l/L varies from 0.32 to 0.60 for $D = 37$ mm. The general trend according to the inter-block spacing is similar to the present experimental results. As displayed in Fig. 12, the resonant frequency based on the traveling time concept closely coincides with the experimental results compared to that by the linear stability theory or by the natural shedding frequency.

If the characteristic length L remains constant while the block length varies, the characteristic frequency of a system cannot be changed by the traveling time concept. Table 2 exhibits the variation of thermal resonance

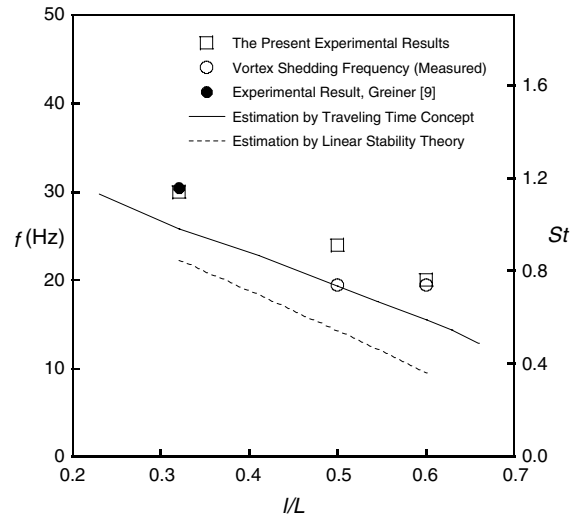


Fig. 12. The effect of inter-block spacing on thermal resonance frequency for $D/a = 4.11$ and $a/H = 0.46$ at $Re_H = 700$ and $A = 0.2$ for the same geometry as Greiner [9].

frequency for various inter-block spacings while the block periodicity is fixed at $L/H = 2.62$. The Reynolds number and the pulsation amplitude are fixed at $Re_H = 232$ and $A = 0.43$, respectively. As anticipated, the thermal resonance frequencies are little changed by the variation of the inter-block spacing for a fixed L . Further, the estimation results are in general accordance with the previous experimental data [11]. The estimation results by the traveling time concept show better agreement with the previous experimental results [11] than the self-sustained oscillation frequency.

Based on the above observation, the traveling time concept can evaluate successfully thermal resonance frequency in a periodic block array channel. The previous estimation based on the linear stability theory and the vortex shedding frequency measurement may not provide appropriate information for thermal resonance frequency.

5. Conclusion

An experimental study has been carried out on the pulsating flow and the associated heat transfer from a

Table 2

Comparison of thermal resonance frequency between the estimation results and the experimental results of Nishimura et al. [11]

Geometry	l/L	L/H	St_R		
			Experimental result [11]	Estimation by traveling time concept	Self-sustained oscillation [11]
G_{N1}	0.33	2.62	0.1275–0.1328	0.1061	0.1018
G_{N2}	0.50	2.62	0.1181–0.1312	0.1061	0.1018

heated block array inside a channel. Impact of the pulsating frequency ($10 \text{ Hz} < f_F < 100 \text{ Hz}$), the velocity amplitude ($A = 0.2$ and 0.3) and the inter-block spacing ($0.33 < l/L < 0.66$) on heat transfer enhancement was investigated.

For the steady flow, the increase of the inter-block spacing augmented the convective heat transfer from the blocks due to increased entrainment of cold fluid. The onset of self-sustained oscillation was also responsible for the heat transfer augmentation for the block array with wider inter-block spacings. A noticeable enhancement in heat transfer was found when the pulsating flow was imposed, depending on the inter-block spacing as well as the pulsation frequency. Heat transfer enhancement at the most upstream block showed a peak at around $f_F = 40 \text{ Hz}$ irrespective of the variation of inter-block spacing. However, thermal resonance frequencies at the downstream blocks decreased with the increase of the inter-block spacing.

To predict thermal resonance frequency for a periodic block array, the traveling time concept was adopted in the present study. St_R is the dimensionless thermal resonance frequency at which the resonance in heat transfer occurs. The thermal resonance frequency predicted by the traveling time concept showed quite good agreement with the experimental data, compared with the previous predictions based on the linear stability theory. Further, thermal resonance frequency did not well coincide with the measured vortex shedding frequency from the blocks.

References

- [1] J. Davalath, Y. Bayazitoglu, Forced convection cooling across rectangular blocks, *ASME J. Heat Transfer* 109 (1987) 321–327.
- [2] S.Y. Kim, H.J. Sung, J.M. Hyun, Mixed convection from multiple-layered boards with cross-streamwise periodic boundary conditions, *Int. J. Heat Mass Transfer* 35 (1992) 2941–2952.
- [3] B. Farhanieh, C. Herman, B. Sundén, Numerical and experimental analysis of laminar fluid flow and forced convection heat transfer in a grooved duct, *Int. J. Heat Mass Transfer* 36 (1993) 1609–1617.
- [4] J.S. Nigen, C.H. Amon, Time-dependent conjugated heat transfer characteristics of self-sustained oscillatory flow in a grooved channel, *ASME J. Fluid Eng.* 116 (1994) 499–507.
- [5] T.J. Young, K. Vafai, Convective flow and heat transfer in a channel containing multiple heated obstacles, *Int. J. Heat Mass Transfer* 41 (1998) 3279–3298.
- [6] T. Furukawa, W. Yang, Thermal-fluid flow in parallel boards with heat generating blocks, *Int. J. Heat Mass Transfer* 46 (2003) 5005–5015.
- [7] N.K. Ghaddar, K.Z. Korczak, B.B. Mikic, A.T. Patera, Numerical investigation of incompressible flow in grooved channels. Part 1. Stability and self-sustained oscillations, *J. Fluid Mech.* 163 (1986) 99–127.
- [8] N.K. Ghaddar, K.Z. Korczak, B.B. Mikic, A.T. Patera, Numerical investigation of incompressible flow in grooved channels. Part 2. Resonance and oscillatory heat-transfer enhancement, *J. Fluid Mech.* 168 (1986) 541–567.
- [9] M. Greiner, An experimental investigation of resonant heat transfer enhancement in grooved channel, *Int. J. Heat Mass Transfer* 34 (1991) 1383–1391.
- [10] S.Y. Kim, B.H. Kang, J.M. Hyun, Forced convection heat transfer from two heated blocks in pulsating channel flow, *Int. J. Heat Mass Transfer* 41 (1998) 625–634.
- [11] T. Nishimura, N. Oka, Y. Yoshinaka, K. Kunitsugu, Influence of imposed oscillatory frequency on mass transfer enhancement of grooved channels for pulsatile flow, *Int. J. Heat Mass Transfer* 43 (2000) 2065–2374.
- [12] J.H. Bae, J.M. Hyun, H.S. Kwak, Mixed convection from a multi-block heater in a channel with imposed thermal modulation, *Num. Heat Transfer* 45 (4) (2004) 329–345.
- [13] C. Loundon, A. Tordesillas, The use of the dimensionless Womersley number to characterize the unsteady nature of internal flow, *J. Theoret. Biol.* 191 (1998) 63–78.
- [14] T.G. Beckwith, R.D. Marangoni, V. Lienhard, *Mechanical Measurements*, Addison Wesley Co Inc., New York, 1995.